

How visual information links to multijoint coordination during quiet standing

J. P. Scholz · E. Park · J. J. Jeka · G. Schöner · T. Kiemel

Received: 3 March 2012 / Accepted: 25 July 2012 / Published online: 25 August 2012
© Springer-Verlag 2012

Abstract The link between visual information and postural control was investigated based on a multi-degree-of-freedom model using the framework of the uncontrolled manifold (UCM) hypothesis. The hypothesis was that because visual information specifies the position of the body in space, it would couple preferentially into those combinations of degrees of freedom (DOFs) that move the body in space and not into combinations of DOFs that do not move the body in space. Subjects stood quietly in a virtual reality cave for 4-min trials with or without a 0.2, 2.0 Hz, or combined 0.2 and 2.0 Hz visual field perturbation that was below perceptual threshold. Motion analysis was used to compute six sagittal plane joint angles. Variance across time of the angular motion was partitioned into (1) variance associated with motion of the body and (2) variance reflecting the use of flexible joint combinations that keep the anterior–posterior positions of the head (HD_{POS}) and center of mass (CM_{POS}) invariant. UCM analysis was performed in the frequency domain in order to

link the sensory perturbation to each variance component at different frequencies. As predicted, variance related to motion of the body was selectively increased at the 0.2-Hz drive frequency but not at other frequencies of sway for both CM_{POS} and HD_{POS} . The dominant effect with the 2.0-Hz visual drive also was limited largely to variance related to motion of the body.

Keywords Visual perception · Multijoint coordination · Uncontrolled manifold · Posture

Introduction

Control of the body center of mass (CM) relative to the base of support is often viewed as the core issue in postural control (Pedrocchi et al. 2002; Peterka 2002; Corrievau et al. 2004; Gage et al. 2004) (but see Kiemel et al. 2011, for an alternative view). To do so requires reasonably accurate estimation of the body's spatial position (i.e., of the CM), which is based on the information from visual, vestibular, and somatosensory senses (Bronstein et al. 1990; Horak and Macpherson 1996; Jeka et al. 2000). A full understanding of the role of sensory estimation for postural stability requires knowledge of the nature of the control system that uses such information to minimize motion of the body relative to the environment. This is true not only for the limited periods during which humans stand quietly, but especially during the performance of more dynamic activities while in standing.

The control of quiet standing is often modeled as control of an inverted pendulum, which has simplified theoretical thinking about postural control considerably (Nashner and McCollum 1985; McCollum and Leen 1989; Nashner et al. 1989; Kuo 1995; Jeka et al. 1998; Winter et al. 1998;

J. P. Scholz (✉) · E. Park
Department of Physical Therapy, 307 McKinly Laboratory,
University of Delaware, Newark, DE 19716, USA
e-mail: jpscholz@udel.edu

J. P. Scholz
Biomechanics and Movement Science Program,
University of Delaware, Newark, DE, USA

J. J. Jeka · T. Kiemel
Department of Kinesiology, University of Maryland,
College Park, MD, USA

G. Schöner
Institut für Neuroinformatik, Ruhr-University,
Bochum, Germany

Loram and Lakie 2002; Peterka 2002; Masani et al. 2006; Maurer et al. 2006). The inverted pendulum hypothesis leads to a unique link between sensory information about the body in space and the degree of freedom that is presumably controlled, that is, motion about the ankle joint. As a result, different sources of sensory information that specify the postural state can be fused. Many influential models of sensory estimation have been developed within this framework (McCullum and Leen 1989; Nashner et al. 1989; Peterka 2002; Masani et al. 2006; Maurer et al. 2006). At the same time, the need to consider more degrees of freedom (DOFs) to adequately understand postural control has been recognized by others (Barin 1989; Jeka et al. 1998; Kuo 1998; Creath et al. 2005). Thus, when analyzed at the kinematic level, DOFs refer to the number of joint motions whose control signals need to be coordinated to achieve a stable postural state. For example, Kuo et al. (1998) showed that altering sensory conditions led to changes in the relative motions of the hip and ankle joints accompanied by changes in postural sway. However, the methods they employed could not determine how much of the measured increase in joint motion actually contributed to postural sway, partly because the motions of only two joints were examined. Indeed, the phrase “postural sway” often refers synonymously to variability of the CM position and of body segments. In the framework of a single inverted pendulum model of posture, segmental motion variability is isomorphic with CM position variability. However, joint or body segment variance may or may not contribute to postural sway when the latter refers to motion of the body in space within a multijoint control scheme (Hsu et al. 2007).

Methodological developments such as the uncontrolled manifold (UCM) approach provide a means to explore the relative contribution of joint motion or muscle activation patterns to postural sway (Scholz and Schönner 1999; Krishnamoorthy et al. 2004, 2005). Recent evidence suggests that multiple joints and muscles along the kinematic chain are actively coordinated to achieve postural control (Horak and Nashner 1986; Kuo 1995; Alexandrov et al. 2005; Creath et al. 2005; Krishnamoorthy et al. 2005; Torres-Oviedo and Ting 2007). For example, an investigation of quiet standing by Hsu et al. (2007) revealed relatively equal variability of joint angles along the body axis, not primarily variability of the ankle and hip joints. Moreover, most of the increased joint variability measured when vision was eliminated during quiet standing did not move the CM substantially. Rather, the increase reflected redundant patterns of joint coordination that achieved the same, mean CM position. Thus, a consideration of ankle motion alone, or even combinations of ankle and hip motion, likely is inadequate to understand mechanisms that stabilize the CM position.

Given that multiple joints along the kinematic chain are active in postural sway during quiet stance (Hsu et al. 2007), a fresh look at the question of how sensory information about the body in space is selectively coupled to the motor control system is required. Sensory information from proprioception and plantar pressure must be linked to sensor information from the head (vision and vestibular) to be interpretable in terms of the body’s position in space (Maurer et al. 2006). Moreover, sensory inputs are inherently noisy (Anastasio and Patton 2004) and sometimes are in conflict. Some models of human postural control have proposed neural versions of Kalman filters to deal with this integration task and the inherent noise of multiple sensory signals (van der Kooij et al. 1999; Kiemel et al. 2002; Kuo 2005). In these models, a Kalman filter continually estimates the body’s position and velocity based on noisy inputs from multiple senses. These estimates could be used to generate appropriate motor commands to stabilize upright stance. The inverted pendulum model postulates a one-to-one relationship between estimates of the kinematic state of the body in space and estimates of the ankle joint position, which is controlled, in turn, to stabilize posture. The inverted pendulum approximation to posture, then, predicts that sensory inputs specifying movement of the environment will generate movement of the CM that is proportional to ankle motion. Two-segment models likewise postulate a one-to-one relationship between body in space and controlled DOFs, leading to the same qualitative prediction. But the process of linking sensory information to control of posture becomes much more complex if the control of many joint DOFs is required to stabilize the body in space (Hsu et al. 2007). Thus, sensory information is clearly tied to the control strategy in ways that are presently not well understood. The goal of the current study was to provide a step in that direction by investigating the extent to which changing sensory information, specifically from vision, affects multi-DOF postural control.

How could the coupling of sensory information about the body in space to multiple DOFs be understood in a way compatible with the findings in quiet stance (Hsu et al. 2007)? A control scheme that directly addresses the control of redundant DOFs has recently been proposed in the context of arm movements (Martin et al. 2009). In that scheme, motor commands related to control of a task-level variable such as the hand’s position are coupled into the range space of the effector, that is, the subspace within which changes in the joint configuration affect the task variable. Conversely, the complementary null space, within which changes of joint configurations do not affect the task variable, is decoupled from such control input. Put another way, to control the hand’s position in space, control signals must be generated to restrict changes in the joint configuration within the range space of that task variable.

In contrast, changes within the null space of the configuration of the same joints not affecting the hand's position could either be restricted or allowed to vary freely. Although simpler from a control perspective, restricting all joint motions reduces flexibility of the effector to accommodate additional task constraints. Indeed, numerous studies have shown that primarily range space motion is restricted to stabilize the hand position while null space motion is significantly larger (Tseng et al. 2002, 2003; Tseng and Scholz 2005).

This control scheme recently was elaborated theoretically for posture (Reimann et al. 2011), assuming a redundant system of joints (Hsu et al. 2007). A prediction is that sensory information about the postural state of the body is coupled selectively into the subspace of joint configurations within which changes in the joint configuration lead to the motion of the body, indexed either by changes in the CM or head position (range space motion). Variance within the range space is often referred to as V_{ORT} . As a result, such sensory information has a much smaller effect on the subspace of joint configurations within which changes do not affect the body's position in space (null space). Variance in the null space is typically referred to as V_{UCM} (see "Methods" section). These predictions led to the experimental hypotheses of this paper: (1) a visual signal that is below subjects' perceptual threshold, and is delivered at a discrete frequency, will lead primarily to an increase in joint variance within the range space (V_{ORT}) while its effect on null space variance (V_{UCM}) will be small or nonexistent; (2) the increase in range space variance compared to quiet standing will be observed primarily at the frequency of the visual signal. Two visual drive frequencies, 0.2 and 2.0 Hz, and their combination constituted three conditions of this study. The frequency of 0.2 Hz is in the range of frequencies of visual flow where strong postural responses have been reported (Kiemel et al. 2006). The 2.0 Hz stimulus was used as a contrast because visual flow at this frequency leads to weaker postural responses and far less power of postural sway exists at this frequency (Creath et al. 2005); (3) Thus, a third hypothesis was that a 2.0 Hz visual drive would have weaker and more diffuse effects on postural sway. These predictions were supported, in part, by the experimental results. In particular, the active insertion of variance into the visual information specifying the position of the body in space primarily affected joint configurations in the range space of joint space. The sensory feedback loop that stabilizes these combinations of DOFs during quiet stance now becomes an additional source of variance. The experimental confirmation of that prediction together with a replication of the previously reported variance effects for quiet stance (Hsu et al. 2007) indicates that this coupling scheme is a viable alternative to the inverted pendulum account for posture.

Methods

Subjects

Fifteen subjects (6 females and 9 males), 22.3 ± 4.15 years old, volunteered to participate in this study. Subjects signed an informed consent form approved by the University of Delaware and University of Maryland Human Subjects Review Board.

Experimental setup

Spherical markers covered with reflective tape were placed at the following locations on the body (Fig. 1a) to track body movement while standing and used to compute sagittal plane joint motion: (1) base of 5th metatarsal of foot; (2) inferior to lateral malleolus; (3) distal lateral condyle of femur; (4) greater trochanter; (5) approximate junction of 5th lumbar and 1st sacral vertebrae: over the left pelvis, approximately 20 % of the distance from the greater trochanter to the shoulder and one-third of the distance from the posterior to anterior iliac spines (de Looze et al. 1992); (6) junction of 7th cervical and 1st thoracic vertebrae; (7) mastoid process; (8) edge of orbital bone lateral to eyeball.

During the experiment, subjects stood on a stationary force platform (Bertec Co., Columbus, OH, USA) while facing into a virtual reality "cave." The subject stood

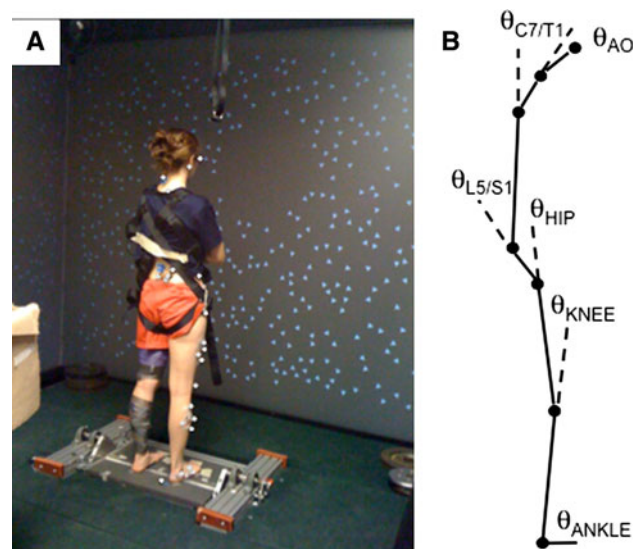


Fig. 1 **a** A photo of the experimental setup. Subjects faced into a virtual cave while focusing their attention on the empty space at the center of an array of triangular bodies that oscillated during the visual perturbation trials. Individual reflective markers were used to estimate sagittal plane joint motion using a link-segment model (see text for details). Rigid bodies, consisting of 3–4 reflective markers each, also were placed on body segments but were not used for the current experimental analyses. **b** Schematic diagram of the sagittal plane joint angles used in the analyses

surrounded by three screens (width, 3.05 m; height, 2.44 m; Fakespace™), one in front of the subject and one on each side. Participants stood 1 m from the front screen, centered between the two side screens. Visual displays were rear-projected to the screens at a frame rate of 60 Hz by JVC projectors (model DLA-M15U; Victor Company of Japan). CaveLib software (Fakespace™) was used to generate a virtual moving visual scene consisting of three walls attached at right angles that coincided with the screens when the visual scene was not moving. Each wall consisted of 500 non-overlapping white small triangles of equal size (approximately $0.2^\circ \times 0.3^\circ \times 0.2^\circ$ of visual angle) with random positions and orientations on a black background. To reduce aliasing effects in the fovea region, no triangles were displayed on the front wall within a 30-cm radius circular region directly in front of the participant's eyes. The display on each screen was varied with time to simulate rotation of the visual scene about the axis through the subject's ankles, assuming a fixed perspective point at the average position of the participant's eyes.

Subjects were asked to assume a foot position on the force plate at the beginning of the experiment with their feet a comfortable distance apart and the forefeet angled outward 14° from the midline (McIlroy and Maki 1997). This position was marked on the force plate with chalk. Subjects then assumed the same foot position on each trial. The instruction to the subjects was to look straight ahead at open area in the screen in front of them.

Experimental conditions

Subjects completed three trials each under four different experimental conditions: (1) Quiet standing while fixating on the open area of the visual display (QSVF) and (2–4) quiet standing while fixating on the open area of the visual display during which the visual display rotated about the ankle joint at (2) 0.2 Hz with an amplitude of 0.2° (VD0.2); (3) at 2.0 Hz with an amplitude of 0.028° (VD2.0); or (4) at a combined frequency of 0.2 and 2.0 Hz (CVD). Each trial of the same condition lasted 4 min. Presentation of the trials was randomized. The combined frequency condition was used to determine whether there were any interactions between the 0.2 and 2.0 Hz frequency components. The applied visual perturbation for conditions 2–4 was below subjects' perceptual threshold to avoid down-weighting of vision that is known to occur with large visual motion amplitude (Jeka et al. 2008).

Data Processing

Movement of the reflective markers was captured at 120 Hz with a VICON™ motion-measurement system composed of eight MX-40 cameras. Ground reaction forces

were recorded at 240 Hz, but are not presented in this report.

Joint angles

Body segment lengths were computed from the reflective markers placed at approximate joint centers along the sagittal plane. Six sagittal plane joint angles (θ_i) then were computed with a link-segment model: (1) ankle, (2) knee, (3) hip, (4) L5-S1 joint, (5) C7-T1 joint, (6) atlanto-occipital (AO) joint (Fig. 1b), using the formula

$$\theta_i = \cos^{-1}(V_1 \cdot V_2)$$

where V_1 and V_2 are unit vectors for the proximal and distal segments, respectively.

Components of joint configuration variance (frequency domain analysis)

The effect of the weak visual perturbations on multijoint coordination was investigated using the UCM approach to motor redundancy (Scholz and Schöner 1999). The method allows joint configuration variance to be partitioned, based on a geometric model relating small changes in joint angles to changes in the values of important performance variables, into two components that have different effects on the values of those performance variables: (1) variance within the null space or UCM subspace of joint space, V_{UCM} , where variable combinations of the joints have no effect on the value of a performance variable and may reflect the use of motor abundance to stabilize that variable; and (2) variance within the range space (V_{ORT}), the subspace of joint space orthogonal to the UCM where variable joint combinations lead to changes of the values of the performance variable. Two performance variables were evaluated in this study, the anterior–posterior (AP) movement of the CM of the body (CM_{POS}) and AP motion of the head in space (HD_{POS}).

Because the visual perturbation occurred at one or two fixed frequencies, UCM analysis was performed in the frequency domain to investigate the effect of the visual perturbation at different frequencies of sway on V_{UCM} and V_{ORT} compared to the QSVF condition. We were particularly interested in the low-frequency components, where most of the power of postural variability lies. The geometric model relating small changes in the joint configuration to changes in the CM_{POS} , which was used to perform frequency domain analysis, is described in the “Appendix”. The geometric model used for variance analysis relative to HD_{POS} was similar, but without the mass locations and mass contributions. The effect of small changes in the joint configuration $\Delta\theta(t)$ on, for example, the

CM_{POS} , is described by the Jacobian \underline{J} , that is, $\Delta r(t) = \underline{J} * \Delta\theta(t)$. We then take the Fourier transform,

$$\begin{aligned}\Delta r(\omega) &= \frac{1}{T} \int_0^T dt * \exp[-i\omega t] * \Delta r(t) \\ &= \frac{1}{T} \int_0^T dt * \exp[-i\omega t] * \underline{J} * \Delta\theta(t)\end{aligned}$$

where T is the length of the trial, ω is frequency, and \int integrates over time; “ i ” is the complex unit. Both $\Delta r(\omega)$ and \underline{J} will differ depending on whether the performance variable is the CM_{POS} or the HD_{POS} . Because \underline{J} does not depend on time under the assumption of quasi-steady-state posture, we have:

$$\Delta r(\omega) = \underline{J} * \frac{1}{T} \int_0^T dt * \exp[-i\omega t] * \Delta\theta(t) = \underline{J} * \Delta\theta(\omega)$$

This equation can be written separately for both real and imaginary parts:

$$\begin{aligned}\Delta r_{REAL}(\omega) &= \underline{J} * \Delta\theta_{REAL}(\omega) \\ \Delta r_{IMAG}(\omega) &= \underline{J} * \Delta\theta_{IMAG}(\omega)\end{aligned}$$

Now, $\Delta\theta(\omega)$ is decomposed by projecting it into the UCM and its complementary orthogonal subspace, as is typical in UCM analysis (Scholz and Schöner 1999), resulting in $\Delta\theta_{UCM}(\omega)$ and $\Delta\theta_{ORT}(\omega)$, respectively. For each frequency bin ω , the variance is then computed within each of these subspaces, and normalized to the number of dimensions of the respective subspace, as

$$V_{UCM}(\omega) = \|\Delta\theta_{UCM}(\omega)\|^2, \quad V_{ORT}(\omega) = \|\Delta\theta_{ORT}(\omega)\|^2,$$

where $\|\cdot\|$ denotes the vector norm.

To have enough data to perform the Fourier deconstruction, this analysis was performed across time within each trial (30,000 data samples). Thus, the Jacobian matrix for each trial was based on the mean joint configuration across the entire trial. Because changes in the joint angles during the trials were relatively minimal, the Jacobian also changed minimally across time, allowing the assumption of a relatively steady-state posture.

Statistical analyses

Most postural sway during quiet standing occurs at frequencies less than 2 Hz (Winter et al. 1998; Zatsiorsky and Duarte 2000; Mochizuki et al. 2006). Therefore, UCM analysis was performed at the two frequencies of the moving visual field, 0.2 and 2.0 Hz, and at frequencies

below 0.2 Hz. This is the case for all conditions, that is, QSVF, VD0.2, VD2.0, and CVD. Thus, three frequency bins are considered in the analysis.

For each performance variable, a two-way, repeated measures multivariate analysis of variance (MANOVA) was performed with V_{UCM} and V_{ORT} as dependent variables and with factors Condition (QSVF, VD0.2, VD2.0, and CVD) and Frequency Bin ($f < 0.2$ Hz, $f = 0.2$ Hz, and $f = 2.0$ Hz). A significant MANOVA was further investigated by examining the univariate effects for each dependent variable and by performing post hoc comparisons with Bonferroni corrections if needed. The primary hypothesis was that the weakly moving visual field would primarily affect body sway at the frequency of the sensory signal, as evidenced by an increase in V_{ORT} , while sway at other frequencies would remain largely unaffected by the visual drive.

Results

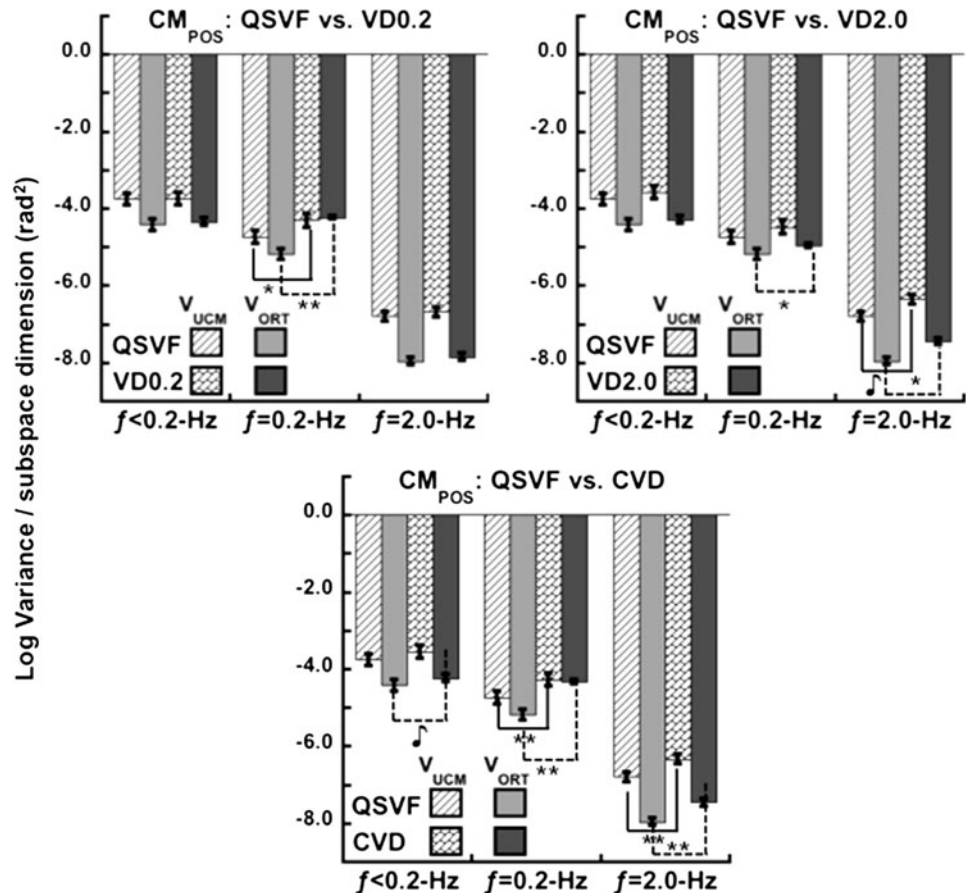
Joint variance related to CM_{POS}

The repeated measures MANOVA revealed significant effects of Condition (QSVF vs. VD0.2 vs. VD2.0: $F_{6,84} = 8.5$, $p < 0.001$), Frequency Bin ($f < 0.2$ Hz vs. $f = 0.2$ Hz vs. $f = 2.0$ Hz: $F_{4,56} = 18.5$, $p < 0.001$) as well as a significant interaction between Condition and Frequency Bin ($F_{12,168} = 31.4$, $p < 0.001$). These three effects were found for both V_{UCM} ($F_{3,42} = 8.3$, $p < 0.001$; $F_{2,28} = 561.6$, $p < 0.001$; $F_{6,84} = 9.4$, $p < 0.001$, respectively) and V_{ORT} ($F_{3,42} = 27.7$, $p < 0.001$; $F_{2,28} = 263.8$, $p < 0.001$; $F_{6,84} = 817.6$, $p < 0.001$, respectively). Because our main interest was in how the added visual drive affected the variance components at different frequencies of sway compared to the QSVF condition, further analyses were performed to investigate the differences between each drive condition and QSVF at each of the three frequency bins.

QSVF versus VD0.2 (Fig. 2, left panel): Adding a 0.2-Hz visual drive to QSVF had no effect on either V_{UCM} ($p > 0.95$) or V_{ORT} ($p > 0.36$) at frequencies below 0.2 Hz (left set of bars). Both V_{UCM} ($F_{1,14} = 15.1$, $p < 0.01$) and V_{ORT} ($F_{1,14} = 118.7$, $p < 0.001$) increased at the drive frequency, however (center set of bars). The increase in V_{ORT} in the 0.2-Hz frequency bin was greater than that for V_{UCM} ($F_{1,14} = 21.4$, $p < 0.001$). No differences were found for either V_{UCM} ($p > 0.26$) or V_{ORT} ($p > 0.08$) at the 2.0 Hz sway frequency when comparing the QSVF and VD0.2 conditions (right set of bars).

QSVF versus VD2.0 (Fig. 2, right panel): With an added 2.0 Hz visual drive (top right panel, Fig. 2), V_{UCM} did not differ between the VD2.0 and QSVF conditions at sway

Fig. 2 Log₁₀ components of joint variance (V_{UCM} and V_{ORT}) related to stability of the AP center of mass position (CM_{POS}) at $f < 0.2$ Hz, $f = 0.2$ Hz, and $f = 2.0$ Hz for quiet standing without a visual perturbation (QSVF) and with a visual field oscillation at 0.2 Hz (VD0.2; left panel), 2.0 Hz (VD2.0; right panel), and with combined 0.2 and 2.0 Hz frequency oscillation (CVD; bottom panel); $^{\dagger}p < 0.05$; $*p < 0.01$; $**p < 0.001$



frequencies below the 2.0 Hz drive frequency ($f < 0.2$ Hz: $p > 0.10$; $f = 0.2$ Hz: $p > 0.08$; left and center set of bars). At the drive frequency, however, V_{UCM} was greater than for the QSVF condition ($F_{1,14} = 11.2$, $p < 0.01$; center set of bars). In contrast to V_{UCM} , V_{ORT} for VD2.0 was significantly or near significantly higher than for QSVF for all frequency bins ($f < 0.2$ Hz: $F_{1,14} = 4.4$, $p = 0.054$; $f = 0.2$ Hz: $F_{1,14} = 13.5$, $p < 0.01$; $f = 2.0$ Hz: $F_{1,14} = 18.9$, $p = 0.001$). The increase of both V_{ORT} and V_{UCM} at 2.0 Hz sway frequency compared to QSVF was similar ($p > 0.52$).

QSVF versus CVD (Fig. 2, bottom panel): Combining the 0.2 and 2.0 Hz visual drives did not affect V_{UCM} at frequencies below 0.2 Hz when compared to the QSVF condition ($p > 0.06$). However, combining the visual drives led to a slight increase in V_{ORT} ($F_{1,14} = 6.0$, $p < 0.05$) at the lower frequencies of sway (left set of bars). Both V_{UCM} and V_{ORT} increased at the 0.2 Hz ($F_{1,14} = 28.4$, $p < 0.001$; $F_{1,14} = 109.4$, $p < 0.001$; center set of bars) and 2.0 Hz ($F_{1,14} = 21.1$, $p < 0.001$; $F_{1,14} = 22.0$, $p < 0.001$; right set of bars) sway frequencies compared to the QSVF condition. The increase at 0.2 Hz sway frequency was greater for V_{ORT} than for V_{UCM} ($F_{1,14} = 13.1$, $p < 0.01$). However, the increase in the variance comparing QSVF to CVD did not

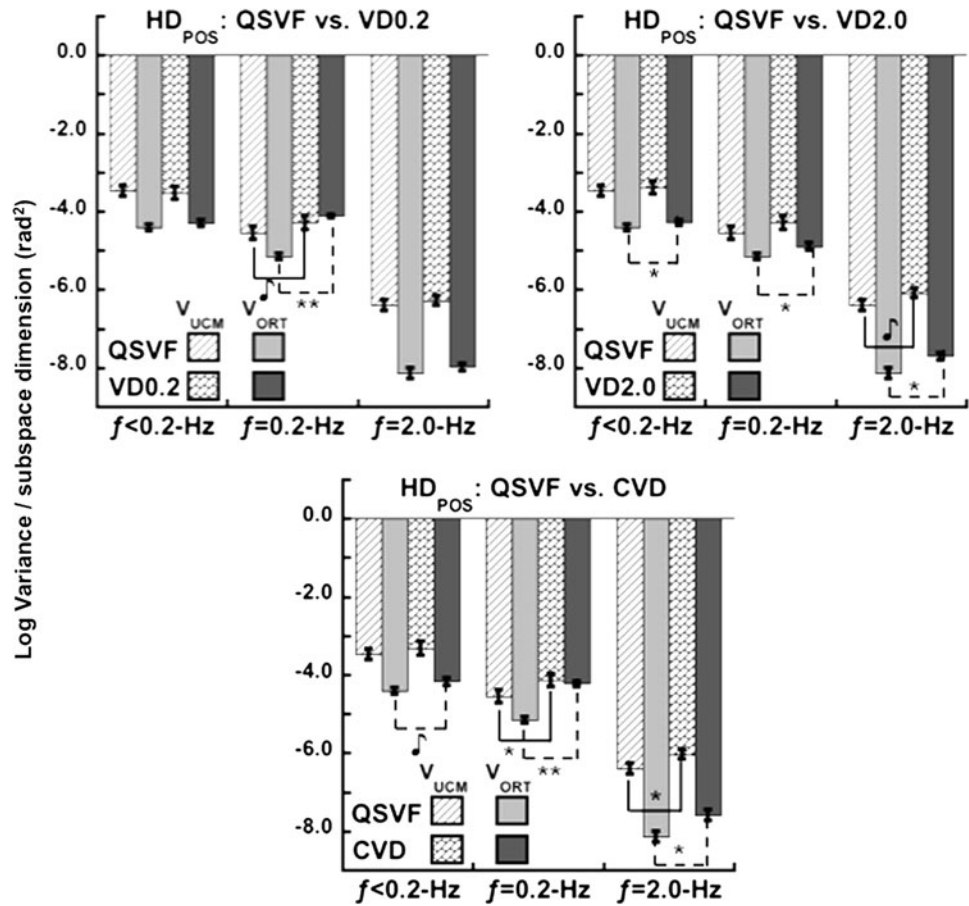
differ between V_{UCM} and V_{ORT} at the 2.0 Hz frequency ($p > 0.71$).

Joint variance related to HD_{POS}

There were significant effects of Condition ($F_{6,84} = 8.8$, $p < 0.001$), Frequency Bin ($F_{4,56} = 30.8$, $p < 0.001$) as well as a significant interaction between Condition and Frequency Bin ($F_{12,168} = 19.8$, $p < 0.001$). These three effects were found for both V_{UCM} ($F_{3,42} = 5.1$, $p < 0.01$; $F_{2,28} = 374.9$, $p < 0.001$; $F_{6,84} = 3.6$, $p < 0.01$, respectively) and V_{ORT} ($F_{3,42} = 29.0$, $p < 0.001$; $F_{2,28} = 268.8$, $p < 0.001$; $F_{6,84} = 666.6$, $p < 0.001$, respectively).

QSVF versus VD0.2 (Fig. 3, left panel): Adding a 0.2-Hz visual drive to QSVF had no effect on either V_{UCM} ($p > 0.54$) or V_{ORT} ($p > 0.09$) at frequencies below 0.2 Hz (left set of bars). Both V_{UCM} ($F_{1,14} = 5.4$, $p < 0.05$) and V_{ORT} ($F_{1,14} = 244.9$, $p < 0.001$) increased at the drive frequency (center set of bars), with the increase in V_{ORT} being larger ($F_{1,14} = 38.3$, $p < 0.001$). No differences were found for either V_{UCM} ($p > 0.21$) or V_{ORT} ($p > 0.11$) at the 2.0 Hz sway frequency when comparing the QSVF and VD0.2 conditions (right set of bars).

Fig. 3 Log₁₀ components of joint variance (V_{UCM} and V_{ORT}) related to stability of the AP head position (HD_{POS}) at $f < 0.2$ Hz, $f = 0.2$ Hz, and $f = 2.0$ Hz for quiet standing without a visual perturbation (QSVF) and with a visual field oscillation at 0.2 Hz (VD0.2; left panel), 2.0 Hz (VD2.0; right panel), and with combined 0.2 and 2.0 Hz frequency oscillation (CVD; bottom panel); $^{\dagger}p < 0.05$; $^*p < 0.01$; $^{**}p < 0.001$



QSVF versus VD2.0 (Fig. 3, right panel): V_{UCM} did not differ between QSVF and VD2.0 when considering sway frequencies lower than 2.0 Hz ($f < 0.2$ Hz: $p > 0.23$; $f = 0.2$ Hz: $p > 0.06$; left and center set of bars). V_{UCM} did increase at the 2.0 Hz drive frequency compared to quiet standing ($F_{1,14} = 7.5$, $p < 0.05$; right set of bars). In contrast to V_{UCM} , adding the 2.0 Hz visual drive to quiet standing led to an increase in V_{ORT} at all frequencies ($f < 0.2$ Hz: $F_{1,14} = 10.7$, $p = 0.01$; $f = 0.2$ Hz: $F_{1,14} = 12.5$, $p < 0.01$; $f = 2.0$ Hz: $F_{1,14} = 18.8$, $p = 0.001$). The increase in V_{ORT} at the 2.0 Hz sway frequency did not differ from the increase in V_{UCM} ($p > 0.18$).

QSVF versus CVD (Fig. 3, bottom panel): Combining the 0.2 and 2.0 Hz visual drives did not affect V_{UCM} at frequencies below 0.2 Hz when compared to the QSVF condition ($p > 0.09$; left set of bars), but did result in an increase in V_{UCM} at both drive frequencies ($f = 0.2$ Hz: $F_{1,14} = 18.1$, $p = 0.001$; $f = 2.0$ Hz: $F_{1,14} = 21.3$, $p < 0.001$; center and right set of bars). Combining the visual drives had a more significant effect on V_{ORT} , leading to an increase over the QSVF condition at all frequencies of sway ($f < 0.02$ Hz: $F_{1,14} = 7.2$, $p < 0.05$; $f = 0.2$ Hz:

$F_{1,14} = 186.5$, $p < 0.001$; $f = 2.0$ Hz: $F_{1,14} = 13.9$, $p < 0.01$). The increase at 0.2 Hz for the CVD condition compared to QSVF was significantly greater for V_{ORT} than for V_{UCM} ($F_{1,14} = 21.9$, $p < 0.001$). The increase over QSVF did not differ between the variance components at the 2.0 Hz sway frequency ($p > 0.14$).

Discussion

The results of this experiment provide some support for Hypotheses 1 and 2. Applying a visual field perturbation that was below subjects' perceptual threshold and at a frequency within the range of typical postural sway (Kiemel et al. 2006) led to a selective increase in joint variance at the drive frequency (0.2 Hz) compared to quiet standing alone. Moreover, a significantly greater increase in joint variance that moves the body in space, that is, V_{ORT} , than variance within the UCM (V_{UCM}), occurred when adding a visual perturbation to quiet standing.

As noted in the introduction, many models of posture have been based on the framework of controlling an inverted pendulum. Although this framework implies a

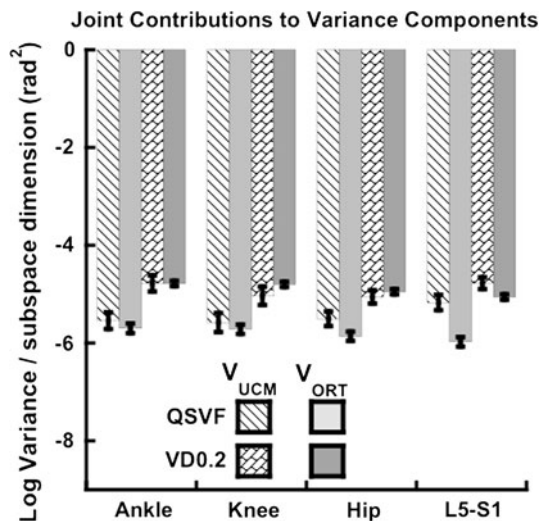


Fig. 4 Log₁₀ components of joint variance (V_{UCM} and V_{ORT}) related to stability of the CM position (CM_{POS}) at $f = 0.2$ Hz for quiet standing without (QSVF) and with a visual field oscillation at 0.2 Hz. In contrast to Fig. 2, the contribution of the four joints included in the CM model to the variance components is illustrated. This was accomplished by re-representing projections of the vector of joint configurations into the UCM subspace and range space back into the original joint space and computing the variances. Note that all joints in quiet standing contribute more to V_{UCM} than to V_{ORT} , including the ankle joint

relatively simplified control scheme (control of the ankle joint) and establishes a direct link between sensory information about the body in space and that control, recent evidence suggests that such a framework is incorrect even for quiet standing. This is because the inverted pendulum hypothesis would predict that most variance should lie in the range space of the body position, onto which the ankle joint primarily loads. Experimentally, however, most variance is found in the null space of body position (Hsu et al. 2007). The results of the current study further emphasize this point. For example, V_{UCM} also was larger than V_{ORT} in the current experiment for all experimental conditions. Consider also the findings illustrated in Fig. 4. This figure compares the UCM results between the QSVF and VD0.2 conditions for CM motion at the frequency of the drive (0.2 Hz). The results are now represented, however, in the full 4-DOF joint space, that is, after projecting the vector of joint configurations into the UCM and range spaces, the lengths of those projections can in turn be projected back into the original joint space and the variances computed. The result provides an indication of how much individual joints contribute to V_{UCM} and V_{ORT} . Two things are noteworthy. First, for all joints, both V_{UCM} and V_{ORT} increased when the visual perturbation was added to quiet standing, although the increase was stronger for V_{ORT} , consistent with the overall findings (Fig. 2). Second, ankle joint

variance in quiet standing contributed more to V_{UCM} than to V_{ORT} . Although this difference decreased when the visual drive was added, reflecting the effect of a moving visual surround on ankle joint motion, the ankle contribution to V_{UCM} was still of similar size as to V_{ORT} . An inverted pendulum model, where motion of the ankle joint is expected to load exclusively on V_{ORT} , would not predict this result. For a two-segment model to reveal a similar pattern of V_{UCM} and V_{ORT} at the ankle, leg (ankle) and trunk segment motions would have to change their relative phase constantly because when the two-segments' motions are in phase or out of phase, either V_{ORT} or V_{UCM} would dominate, respectively. Indeed, based on previous studies of leg–trunk motion (Creath et al. 2005), relative motion between the leg and trunk up to 1.0 Hz is in phase.

How can the coupling of sensory information about the body in space to multiple DOFs be understood in a way compatible with the findings in quiet stance? As discussed in the Introduction, a theoretical control scheme that directly addresses the control of redundant DOFs was proposed recently in the context of arm movements (Martin et al. 2009) and has been extended to postural control (Reimann et al. 2011). Rather than stiffen all joints proximal to the ankle as proposed by an inverted pendulum model, this model is based on a neural network that decouples the space of configurations of multiple joints that affect the body's position (range space) from configurations of the same joints that do not (UCM subspace or null space). The control law that implements this decoupling also limits the effect of sensory information about the body's position in space to the range space. In other words, the gains of feedback loops that act on the range space are high while the gains of those feedback loops that act on the UCM subspace are low. Thus, sensory information couples selectively into the range space so that when a subthreshold visual perturbation is provided that specifies movement of the body, feedback loops related to vision will act to move the body in the opposite direction, introducing variance within the range space. In situations where the external environment is not moving, unplanned sway of the whole body will be constrained by the high gain of the feedback loops. At the same time, any variance induced within the UCM will only be constrained weakly.

In simulations of this model, Reimann et al. (2011) showed that increasing “neural” noise, that is, reflecting noise in the neural network that maps virtual joint (λ) velocities (Feldman and Levin 1995) onto velocity of the body in space led to a selective increase in V_{UCM} . In contrast, increasing sensory noise, reflecting noisy sensors, led to variance that was mostly within the range space, that is, V_{ORT} , a result consistent with those of the current experiments. Although the system being controlled within this framework consists of multiple DOFs, sensory

information is coupled not to individual DOFs but instead to the neural equivalent of the range space, that is, changes of the joint configuration within this subspace still specifies one-dimensional movement with respect to the AP position of the head or CM and can be linked in a similar way to changes in sensory channels related to the body's movement in space along that dimension, not unlike the inverted pendulum model.

The fact that increases in joint variance within the UCM occurred when a subthreshold visual perturbation was added to quiet standing could also be understood within this model (Martin et al. 2009; Reimann et al. 2011). As already noted, the gains of the feedback loops in the model are low within the UCM subspace but not zero. Thus, some variance within the UCM could be expected. Moreover, Martin et al. (2009) compared their UCM model of reaching to an account in which an internal model compensates perfectly for mechanical interactions along the kinematic chain. They found that the latter type of model failed to account for the observed experimental differences between V_{UCM} and V_{ORT} . Thus, the decoupling of the two subspaces of joint configurations likely is imperfect. In addition, results from the condition that involved the 2.0 Hz frequency were not as selective. Although changes in V_{UCM} were still limited to the drive frequency, V_{ORT} increased more or less compared to quiet standing at all frequencies tested for both HD_{POS} and CM_{POS} . Thus, adding a visual perturbation at a frequency above those where most of the power of sway resides had a more general effect on joint variance related to motion of the body in space.

A possible explanation for the less selective response of V_{ORT} at the higher drive frequency could be the higher velocity of this visual signal. Most work reporting down-weighting of specific sensory stimuli manipulated the amplitude of the stimulus. For example, an increase in the amplitude of environmental motion is accompanied by a corresponding decrease in gain of postural compensation (Peterka and Benolken 1995; Oie et al. 2002; Peterka 2002). The consequence of down-weighting vision was found to be higher variability of sway at frequencies other than the drive due to reduced sensory information available for posture estimation (Jeka et al. 2008). Less is known about the effect of different drive frequencies on sensory weighting. However, the amplitude values chosen for the visual drive in the current experiment also resulted in a higher velocity of the 2.0 Hz visual drive. Given that velocity information appears to be more salient than position information for controlling posture (Jeka et al. 2004), it is possible that the higher velocity of the signal led to some down-weighting of visual information, which could account for the spread of V_{ORT} across all frequency bins. Therefore, further investigation is needed that better

controls for the velocity of the visual signal to determine whether this explanation is correct. Another possibility is that muscle noise has a stronger effect on higher frequencies of postural sway (Reimann et al. 2011). However, muscle noise was also found in the model to have relatively equal effects on both variance components.

The results of this study reveal an important link between the sensory information specifying upright posture and the multi-DOF control system and are consistent with the UCM control hypothesis (Scholz and Schöner 1999; Reimann et al. 2011). Linking sensory information selectively into the subspace of effector space that leads to motion of the body in space helps to solve the multi-DOF control problem. Within this framework, sensory signals related to motion of the body in space have minimal influence on combinations of effectors that do not move the body in space. Instead, sensory information is linked more strongly to the subspace of the effectors that leads to body motion. In the case of a pure perturbation, the link of sensory information into the subspace orthogonal to the UCM can serve to drive appropriate changes in posture. In the current experiment, the subconscious visual information specified falling forward or backward, so adjustments of posture, reflected by increased V_{ORT} , are appropriate. In other cases not investigated here, it may be more appropriate to restrict motion in that subspace, perhaps when the sensory information specifies motion of the body created by volitional actions. Further investigation is clearly needed in a variety of contexts but the current results provide a starting point for understanding how sensory information about posture can be linked to a multi-DOF control system.

Acknowledgments This research was supported by the Grant 0957920, awarded to John Scholz and John Jeka from the National Science Foundation and Grant Scho336/7-1 from the Deutsche Forschungsgemeinschaft awarded to Gregor Schöner.

Appendix

The geometric model of the standing configuration related to the AP center of mass position (CM_{POS}) in the sagittal plane was formulated in terms of four joint angles (θ_i), where $i = [\text{ankle, knee, hip, and L5-S1}]$, and four limb segment lengths (l_j), the proportion of mass each contributes to the total body mass (m_j), and the distance of the individual segment masses from the distal end of the segment (d_j), where for all $j = [\text{shank (SH), thigh (TH), pelvis (PV), head–arms–trunk (HAT)}]$ (Winter 2009).

The geometric model for CM motion in the AP dimension is:

$$\begin{aligned}
 d_{CM} = & m_{SH} * d_{SH} * l_{SH} * \cos(\theta_{ANKLE}) \\
 & + \dots m_{TH} * (l_{SH} * \cos(\theta_{ANKLE}) \\
 & + l_{TH} * d_{TH} * \cos(\theta_{ANKLE} + \theta_{KNEE})) \\
 & + \dots m_{PV} * (l_{SH} * \cos(\theta_{ANKLE}) \\
 & + l_{TH} * \cos(\theta_{ANKLE} + \theta_{KNEE}) \\
 & + l_{PV} * d_{PV} * \cos(\theta_{ANKLE} + \theta_{KNEE} + \theta_{HIP})) \\
 & + \dots m_{HAT} * (l_{SH} * \cos(\theta_{ANKLE}) \\
 & + l_{TH} * \cos(\theta_{ANKLE} + \theta_{KNEE}) \\
 & + l_{PV} * \cos(\theta_{ANKLE} + \theta_{KNEE} + \theta_{HIP}) \\
 & + l_{HAT} * d_{HAT} * \cos(\theta_{ANKLE} + \theta_{KNEE} \\
 & + \theta_{HIP} + \theta_{L5/S1})).
 \end{aligned}$$

The geometric model for head motion in the AP dimension is:

$$\begin{aligned}
 d_{HD} = & l_{SH} * \cos(\theta_{ANKLE}) \\
 & + \dots l_{TH} * \cos(\theta_{ANKLE} + \theta_{KNEE}) \\
 & + \dots l_{PV} * \cos(\theta_{ANKLE} + \theta_{KNEE} + \theta_{HIP}) \\
 & + \dots l_{TRUNK} * \cos(\theta_{ANKLE} + \theta_{KNEE} + \theta_{HIP} + \theta_{L5/S1}) \\
 & + \dots l_{NECK} * \cos(\theta_{ANKLE} + \theta_{KNEE} \\
 & + \theta_{HIP} + \theta_{L5/S1} + \theta_{C7/T1}) \\
 & + \dots l_{HEAD} * \cos(\theta_{ANKLE} \\
 & + \theta_{KNEE} + \theta_{HIP} + \theta_{L5/S1} + \theta_{C7/T1} + \theta_{AO}).
 \end{aligned}$$

Jacobian matrices were obtained by computing analytically for each equation the partial derivative with respect to each joint angle, for example,

$$\begin{aligned}
 \partial_{CM} / \partial_{\theta_{ankle}} = & - m_{SH} * d_{SH} * l_{SH} * \sin(\theta_{ANKLE}) - m_{TH} \\
 & * l_{SH} * \sin(\theta_{ANKLE}) - m_{TH} * l_{TH} * d_{TH} \\
 & * \sin(\theta_{ANKLE} + \theta_{KNEE}) \\
 & - m_{PV} * l_{SH} * \sin(\theta_{ANKLE}) - m_{PV} \\
 & * l_{TH} * \sin(\theta_{ANKLE} + \theta_{KNEE}) - m_{PV} * l_{PV} \\
 & * d_{PV} * \sin(\theta_{ANKLE} + \theta_{KNEE} + \theta_{HIP}) \\
 & - m_{HAT} * l_{SH} * \sin(\theta_{ANKLE}) - m_{HAT} \\
 & * l_{TH} * \sin(\theta_{ANKLE} + \theta_{KNEE}) - m_{HAT} \\
 & * l_{PV} * \sin(\theta_{ANKLE} + \theta_{KNEE} + \theta_{HIP}) \\
 & - m_{HAT} * l_{HAT} * d_{HAT} * \sin(\theta_{ANKLE} \\
 & + \theta_{KNEE} + \theta_{HIP} + \theta_{L5/S1}).
 \end{aligned}$$

References

Alexandrov AV, Frolov AA, Horak FB, Carlson-Kuhta P, Park S (2005) Feedback equilibrium control during human standing. *Biol Cybern* 93:309–322
 Anastasio T, Patton P (2004) Analysis and modeling of multisensory enhancement in the deep superior colliculus. In: Calvert G, Spence C, Stein BE (eds) *Handbook of multisensory processes*. MIT Press, Boston

Barin K (1989) Evaluation of a generalized-model of human postural dynamics and control in the sagittal plane. *Biol Cybern* 61:37–50
 Bronstein AM, Hood JD, Gresty MA, Panagi C (1990) Visual control of balance in cerebellar and parkinsonian syndromes. *Brain* 113:767–779
 Corriveau H, Hebert R, Raïche M, Dubois MF, Prince F (2004) Postural stability in the elderly: empirical confirmation of a theoretical model. *Arch Gerontol Geriatr* 39:163–177
 Creath R, Kiemel T, Horak FB, Peterka RJ, Jeka JJ (2005) A unified view of quiet and perturbed stance: simultaneous co-existing excitable modes. *Neurosci Lett* 377:75–80
 de Looze MP, Kingma I, Bussmann JBJ, Toussaint HM (1992) Validation of a dynamic linked segment model to calculate joint moments in lifting. *Clin Biomech* 7:161
 Feldman AG, Levin MF (1995) The origin and use of positional frames of reference in motor control. *Behav Brain Sci* 18:723–806
 Gage WH, Winter DA, Frank JS, Adkin AL (2004) Kinematic and kinetic validity of the inverted pendulum model in quiet standing. *Gait Posture* 19:124–132
 Horak FB, Macpherson JM (1996) Postural orientation and equilibrium. In: Shepard J, Rowell L (eds) *Handbook of physiology*. Oxford University Press, New York, pp 255–292
 Horak FB, Nashner LM (1986) Central programming of postural movements: adaptation to altered support-surface configurations. *J Neurophysiol* 55:1369–1381
 Hsu WL, Scholz JP, Schoner G, Jeka JJ, Kiemel T (2007) Control and estimation of posture during quiet stance depends on multijoint coordination. *J Neurophysiol* 97:3024–3035
 Jeka JJ, Oie K, Schoner G, Dijkstra T, Henson E (1998) Position and velocity coupling of postural sway to somatosensory drive. *J Neurophysiol* 79:1661
 Jeka JJ, Oie KS, Kiemel T (2000) Multisensory information for human postural control: integrating touch and vision. *Exp Brain Res* 134:107–125
 Jeka J, Kiemel T, Creath R, Horak FB, Peterka R (2004) Controlling human upright posture: velocity information is more accurate than position or acceleration. *J Neurophysiol* 92:2368–2379
 Jeka JJ, Oie KS, Kiemel T (2008) Asymmetric adaptation with functional advantage in human sensorimotor control. *Exp Brain Res* 191:453–463
 Kiemel T, Oie KS, Jeka JJ (2002) Multisensory fusion and the stochastic structure of postural sway. *Biol Cybern* 87:262–277
 Kiemel T, Oie KS, Jeka JJ (2006) Slow dynamics of postural sway are in the feedback loop. *J Neurophysiol* 95:1410–1418
 Kiemel T, Zhang Y, Jeka JJ (2011) Identification of neural feedback for upright stance in humans: stabilization rather than sway minimization. *J Neurosci* 31:15144–15153
 Krishnamoorthy V, Latash ML, Scholz JP, Zatsiorsky VM (2004) Muscle modes during shifts of the center of pressure by standing persons: effect of instability and additional support. *Exp Brain Res* 157:18
 Krishnamoorthy V, Yang J-F, Scholz JP (2005) Joint coordination during quiet stance: effects of vision. *Exp Brain Res* 164:1–17
 Kuo AD (1995) An optimal control model for analyzing human postural balance. *IEEE Trans Biomedical Eng* 42:87–101
 Kuo AD (1998) A least-squares estimation approach to improving the precision of inverse dynamics computations. *J Biomech Eng* 120:148
 Kuo AD (2005) An optimal state estimation model of sensory integration in human postural balance. *J Neural Eng* 2:S235–S249
 Kuo AD, Speers RA, Peterka RJ, Horak FB (1998) Effect of altered sensory conditions on multivariate descriptors of human postural sway. *Exp Brain Res* 122:185–195
 Loram ID, Lakie M (2002) Direct measurement of human ankle stiffness during quiet standing: the intrinsic mechanical stiffness is insufficient for stability. *J Physiol* 545:1041–1053

- Martin V, Scholz JP, Schöner G (2009) Redundancy, self-motion and motor control. *Neural Comput* 21:1371–1414
- Masani K, Vette AH, Popovic MR (2006) Controlling balance during quiet standing: proportional and derivative controller generates preceding motor command to body sway position observed in experiments. *Gait Posture* 23:164–172
- Maurer C, Mergner T, Peterka RJ (2006) Multisensory control of human upright stance. *Exp Brain Res* 171:231–250
- McCollum G, Leen TK (1989) Form and exploration of mechanical stability limits in erect stance. *J Mot Behav* 21:225–244
- McIlroy WE, Maki BE (1997) Preferred placement of the feet during quiet stance: development of a standardized foot placement for balance testing. *Clin Biomech* 12:66–70
- Mochizuki L, Duarte M, Amadio AC, Zatsiorsky VM, Latash ML (2006) Changes in postural sway and its fractions in conditions of postural instability. *J Appl Biomech* 22:51–60
- Nashner LM, McCollum G (1985) The organization of human postural movements: a formal basis and experimental synthesis. *Behav Brain Sci* 8:135–172
- Nashner LM, Shupert CL, Horak FB, Black FO (1989) Organization of posture controls: an analysis of sensory and mechanical constraints. *Prog Brain Res* 80:411–418
- Oie KS, Kiemel T, Jeka JJ (2002) Multisensory fusion: simultaneous re-weighting of vision and touch for the control of human posture. *Cogn Brain Res* 14:164–176
- Pedrocchi A, Baroni G, Mouchnino L, Ferrigno G, Pedotti A, Massion J (2002) Absence of center of mass control for leg abduction in long-term weightlessness in humans. *Neurosci Lett* 319:172–176
- Peterka RJ (2002) Sensorimotor integration in human postural control. *J Neurophysiol* 88:1097–1118
- Peterka RJ, Benolken MS (1995) Role of somatosensory and vestibular cues in attenuating visually induced human postural sway. *Exp Brain Res* 105:101–110
- Reimann H, Schöner G, Scholz JP (2011) Visual information is sufficient for maintaining upright stance—a multi-joint model of human posture. In: 41st Annual meeting of the Society for Neuroscience, vol 184.05/RR1. Washington Convention Center, Washington, DC
- Scholz JP, Schöner G (1999) The uncontrolled manifold concept: identifying control variables for a functional task. *Exp Brain Res* 126:289–306
- Torres-Oviedo G, Ting LH (2007) Muscle synergies characterizing human postural responses. *J Neurophysiol* 98:2144–2156
- Tseng YW, Scholz JP (2005) The effect of workspace on the use of motor abundance. *Mot Control* 9:75–100
- Tseng Y, Scholz JP, Schöner G (2002) Goal-equivalent joint coordination in pointing: affect of vision and arm dominance. *Mot Control* 6:183–207
- Tseng YW, Scholz JP, Schöner G, Hotchkiss L (2003) Effect of accuracy constraint on joint coordination during pointing movements. *Exp Brain Res* 149:276–288
- van der Kooij H, Jacobs R, Koopman B, Grootenboer H (1999) A multisensory integration model of human stance control. *Biol Cybern* 80:299–308
- Winter DA (2009) *Biomechanics and motor control of human movement*. Wiley, Hoboken
- Winter DA, Patla AE, Prince F, Ishac M, Gielo-Perczak K (1998) Stiffness control of balance in quiet standing. *J Neurophysiol* 80:1211–1221
- Zatsiorsky VM, Duarte M (2000) Rambling and trembling in quiet standing. *Mot Control* 4:185